Using several monitoring techniques to measure the rock mass deformation in the Montserrat Massif

Using several monitoring techniques to measure the rock mass deformation in the Montserrat Massif

M Janeras[1]**, JA Jara**[1]**, F López**[1]**, J Marturià**[1]**, MJ Royán**[2]**, JM Vilaplana**[2]**, A Aguasca**[3]**, X Fàbregas**[3]**, F Cabranes**[4]**, JA Gili**[4]

[1] Institut Cartogràfic i Geològic de Catalunya (ICGC), Parc de Montjuïc, 08038-Barcelona, Spain
[2] RISKNAT Group, GEOMODELS. Department of Geodynamics and Geophysics, Faculty of Geology, University of Barcelona (UB), 08028-Barcelona, Spain
[3] RSLAB - Research Group on Remote Sensing. Signal Theory and Communications Department, Technical University of Catalonia (UPC), 08034-Barcelona, Spain
[4] Department of Geotechnical Engineering and Geosciences, Technical University of Catalonia (UPC), 08034-Barcelona, Spain

E-mail: marc.janeras@icgc.cat

Abstract. Montserrat Mountain is located near Barcelona in Catalonia, at the north-east corner of Spain, and its massif is formed by conglomerate interleaved by siltstone/sandstone with steep slopes very prone to rock falls. The increasing visitor's number in the monastery area, reaching 2.4 million per year, has pointed out the risk derived from rock falls for this building area and also for the terrestrial accesses, both roads and rack railway. A risk mitigation plan is currently been applied for 2014-2016 that contains monitoring testing and implementation as a key point. The preliminary results of the pilot tests carried out during 2014 are presented, also profiting from previous sparse experiences and data, and combining 4 monitoring techniques under different conditions of continuity in space and time domains, which are: displacement monitoring with Ground-based Synthetic Aperture Radar and characterization at slope scale, with an extremely non uniform atmospheric phase screen because of the stepped topography and atmosphere stratification; Terrestrial Laser Scanner surveys quantifying frequency for unnoticed activity of small rock falls, and monitoring rock block displacements over 1cm; monitoring of rock joints with a wireless net of sensors; and tentative surveying for singular rocky needles with Total Station.

1. Introduction

1.1. Situation and background

Montserrat Mountain is located near Barcelona in Catalonia, at the north-east corner of Spain (figure 1). This isolated massif formed by thick layers of conglomerate interleaved by siltstone/sandstone coming from a Late-Eocene fan-delta, emerges over the Llobregat River with an overall height of 1000 m (from 200 to 1200 m.a.s.l.). This configuration leads to staggered slopes where vertical cliffs of conglomerate alternate with steep slopes (figure 2). The slight tectonic suffered by this massif preserved the horizontality of the stratigraphic layers, but also determined two dominant joint sets which are planar, vertical, orthogonal, very persistent and with spacing usually ranging from

1 – 10 m [1]. A main consequence of this geological structure is that the massif is very prone to rock falls.

Figure 1. Situation map of Montserrat in Catalonia, NE corner of Spain.

Figure 2. Overview of Montserrat Monastery area and the access by road and railway (SE edge of Montserrat Mountain).

Montserrat massif constitutes a Natural Park (about 3500 ha) and hosts a sanctuary and monastery with a millenarian history and great tradition in Catalonia. The monastery and some touristic premises are placed at the SE edge of the mountain at 700 m.a.s.l. Combining the local and foreign tourism or pilgrimage, the visitor's number in the monastery area is increasing yearly, reaching 2.4 million per year in 2014. Leaving aside this focus, nowadays it is estimated that an additional 0.8 million person per year are circulating for hiking or climbing overall Natural Park.

These hazardous conditions, faced to the concentrated exposition, point out the risk derived from rock falls for this building area and also for the terrestrial accesses, both roads and rack railway ([2], [3] and figure 2).

1.2. Rock fall risk

In this particular massif, rock mass instabilities range 6 orders of magnitude in volume, starting with pebbles disaggregation in the conglomerate, following with slabs and plates, and ending with monolithic rock masses (1000 m^3 or more) delimited by spaced joints. Several recent episodes have highlighted that the frequency is higher than social perception tends to recognize. After [4] and [5], a frequency of about 10 rockfall per year is estimated for magnitude over few tens cubic meters in the overall mountain massif.

In the period 2001-2014, several active and passive protection works have been carried out, mainly along railway and, after several major rock falls, also for the road access. In 2014 a new 3-year plan for global risk mitigation has been started. It is founded by the Catalan Government, directed by Institut Cartogràfic i Geològic de Catalunya (ICGC, the public service for cartography and geology), and supervised by the Patronat de la Muntanya de Montserrat (PMM, the public entity that manages this natural and cultural heritage, under protection) [6].

Figure 3. 2008/12/28 and 890 m^3 rockfall event at Degotalls cliff (right). In the left-hand pictures, the road and the railway cut by blocks can be appreciated.

For the larger events, stabilization measures are only possible in some specific cases; also passive defences, like rock fall fences, offer only partial protection for low magnitude rock falls. Therefore, monitoring is explored as a new line of work in Montserrat, while not feasible as an early warning system (EWS) at present state of experience in site, at least to improve the knowledge on the failure triggering factors, which is a main goal adopted for the current risk mitigation plan at short term. The aim of this hazard control strategy is to get an aid for setting priorities for stabilization works, that might achieve a fairly and sustainable risk management.

In this sense, successive rock falls between 2007 and 2008 at the same place (a 170m high cliff called Degotalls, figure 3) remarked the importance to detect the progression of fractures in the rock mass, and therefore the need of monitoring rock mass deformation and a better comprehension of the instability mechanisms.

2. Monitoring techniques

Landslides are commonly monitored and several early warning systems are implemented successfully, thanks to the displacements of the terrain that often are developed along a certain period before collapse. References about premonitory deformations of rockfall are ever more usual as [7] and [8]. In the Montserrat case, considering the properties of the rock mass, it can be especially difficult to implement such type of approach because the mechanical behaviour seems to be very stiff and/or brittle; the collapse can be reached at low strain. For this reason, high precision measurements will be mandatory. The goal of monitoring action during the current 3-year plan is to improve the knowledge on rock mass behaviour and the comprehension of the instability propagation and the failure preparation, like in [9] and [10]. Thus, in this first current phase different pilot tests are being performed to check the applicability of several techniques depending on each case and site.

To carry out this project, ICGC has established scientific-technical collaboration with specialized research teams of UPC (Technical University of Catalonia) and UB (University of Barcelona). After the analysis and comparison of these first results, new monitoring tests are under study and development for 2015-16. For the first current phase, 4 monitoring techniques were selected with different spatial resolution (punctual or scattered) and temporal acquisition (continuous or discontinuous) as seen in table 1. These 4 techniques and each test performed in Montserrat during

2014 are introduced in next subsections 2.1 to 2.4, but their preliminary results will be summarized in common in section 3.

Table 1. Overview of the 4 monitoring techniques used in the pilot tests.

		Temporal domain	
		Continuous	Discontinuous
Spatial domain	Scattered	Ground Based Synthetic Aperture Radar	Terrestrial Laser Scanner
	Punctual	Rock joint instrumentation	Total Station

2.1. Surveying Total Station

The monitoring with Total Station (figure 4) is the simplest technique presented in this contribution. It was envisaged as a very cheap (low cost) approach to monitor a small number of points in a block. The initial approach is also punctual in the time domain as the measurements are carried out by campaigns through periodic visits.

The Cadireta block (figure 5) was used as a demonstration place to adapt the method and assess its performance. It is a block about 8000 m³ that is overhanging over the hillslope. Its potential risk only threatens a number of trails and the mountain-climbers visiting the area, and the local road that surrounds the Mountain [11]. Here, our main goal has been to test the monitoring method.

Figure 4. Leica TM30 Total Station used in Montserrat, and lateral view of the Cadireta and the base station (in the road).

A convenient place for setting up the Total Station was the small road bellow the block (figure 4). From there, the measurements were made over a set of prisms distributed over the block and around it (attached to the rear wall, used as references, see figure 6).

Figure 5. The Cadireta block in the Montserrat north face, in the "Agulles" (needles) zone.

As expected, the big slope-distances between the Total Station and the block (520-540 m) prevented to reach a high precision in the coordinates of the prisms (XYZ). The angular precision (about 1 arc second, i.e. 0.3 mgon) produced a significant error in the coordinates (3 to 5 mm). On the other hand, the measured distance is more robust (in the mm-level).

So, the distance difference between points ($D_{ij} = D_i - D_j$) is being used as monitoring observable (figure 4 and 6). D_i is the distance to a control prism, whereas D_j is the distance to the closer reference prism. Several tests have been carried out at the Cadireta site to confirm the actual precision of the method. The results show that the Standard Deviation of ΔD_{ij} is close to 0.8 mm, whereas the Standard Deviation of the 3D coordinates is roughly 5 mm.
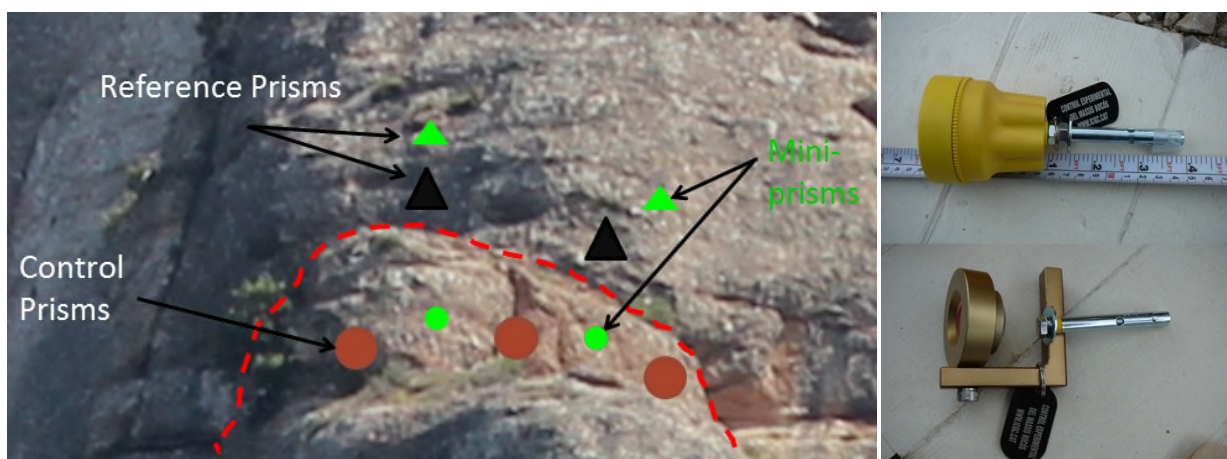

Figure 6. Close view of the top part of the Cadireta block (contoured by dashed red line). The prisms are attached to the block and also to the rear wall (used as reference). Right: standard circular prism or reflector (top) and mini-prism (bottom).

Moreover, this differential procedure has two additional advantages. The first one is related with the correction of the raw distances to take into account the ambient factors. In the Montserrat

Mountain it is very difficult to measure the actual temperature and humidity of the air due to its huge variability in time and in elevation, like exposed in section 2.4 as a critical factor for GBSAR. Through the difference of similar measurements, the observable is quite insensitive to small inaccuracies in the measurement /estimation of the mean temperature and humidity along the laser beam. Secondly, our procedure is also robust in front of small "changes" in the base point; these spurious "movement" might be produced by an eccentricity in the setup of the Total Station or by a real settlement of the ground in the vicinity of the base benchmark.

When writing this contribution we have just acquired the firsts campaigns at the Cadireta site; we plan to carry out a seasonal monitoring during some years in order to characterize the natural behaviour of this block. On the other hand, we plan to spread this simple methodology to other points around the Mountain in order to crosscheck the other techniques.

2.2. Monitoring of rock joints

Monitoring of rock mass movement by installing sensors that directly measure the relative motion of discrete points of individualized blocks is a method of monitoring; when combined with an automatic data acquisition system, the method can provide high precision data and high temporal resolution in real time.

In Montserrat, an experience with this ausculation technique was started on September 2010 to monitor the movement of a huge rock mass (A3-6 block). To that end, 3 displacement extensometric type sensors together with an air temperature sensor were installed to measure movement of this mass relative to the massif. These sensors were wire-connected to a CR800 Campbell Scientific (CS) datalogger provided with a photovoltaic power system and a 3G mobile communications system for remote access. Data are acquired at one sample per minute and stored locally every 30 minutes. This system provides continuous data with ±0.01 mm of resolution and ±0.02 mm of precision.

Currently, after four and a half years of operation, system continues providing continuous data demonstrating its feasibility for long term operation. Some results will be given in section 3.2. Data show elastic displacements, with a full range of about 2.5 mm, clearly related with thermal effects on mass and sensors. However, a major disadvantage of such auscultation technique is the effort, and the cost, of cabling the sensors until the datalogger, especially at Montserrat massif where this task must be carried out by personnel qualified for rope access works.

A project to extend auscultation in Montserrat massif to others potentially unstable blocks was started in 2014, following the priorities previously analysed in [6] and [12]. Taking advantage of experience with A3-6 block, new sensors were installed along the year to monitor the movement of a cluster of blocks called "devil's ceiling" (Diable), where a huge rockfall occurred in XVIth century, as from historical documents (figure 7).

Three different types of displacement sensors have been installed: 13 crackmeters to measure distances between close anchor points (figure 8a), 5 wire crackmeters to measure distances between distant anchor points and 4 tiltmeters, based on MEMS accelerometers, mounted on aluminium beams to measure vertical displacement between anchor points of the beam (figure 8b).
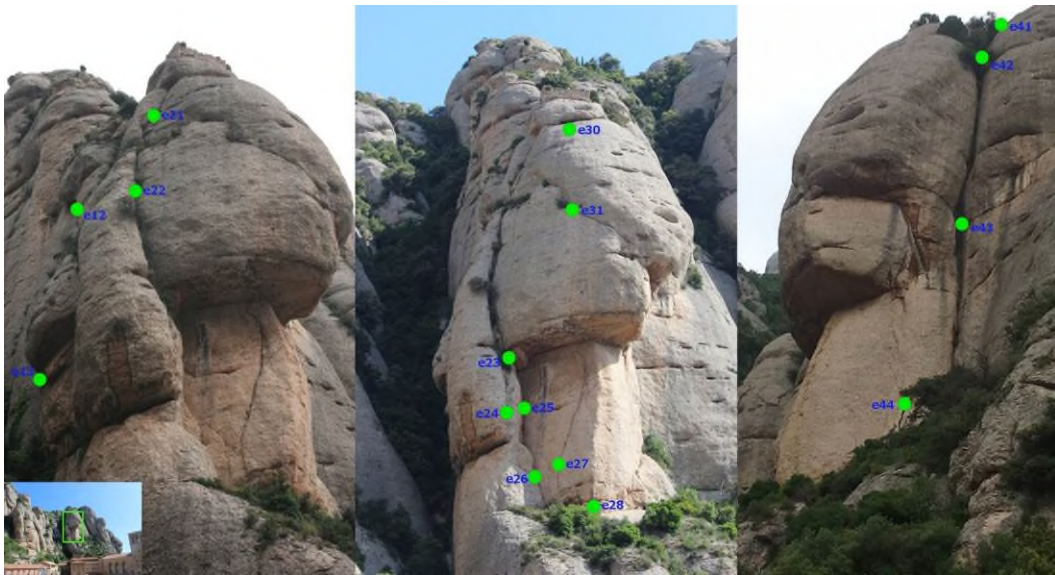
Figure 7. Situation, front and side views of the cluster of blocks called "devil's ceiling" at Montserrat massif. Green spots illustrate the locations of the installed sensors. Each spot represents one or more sensors.
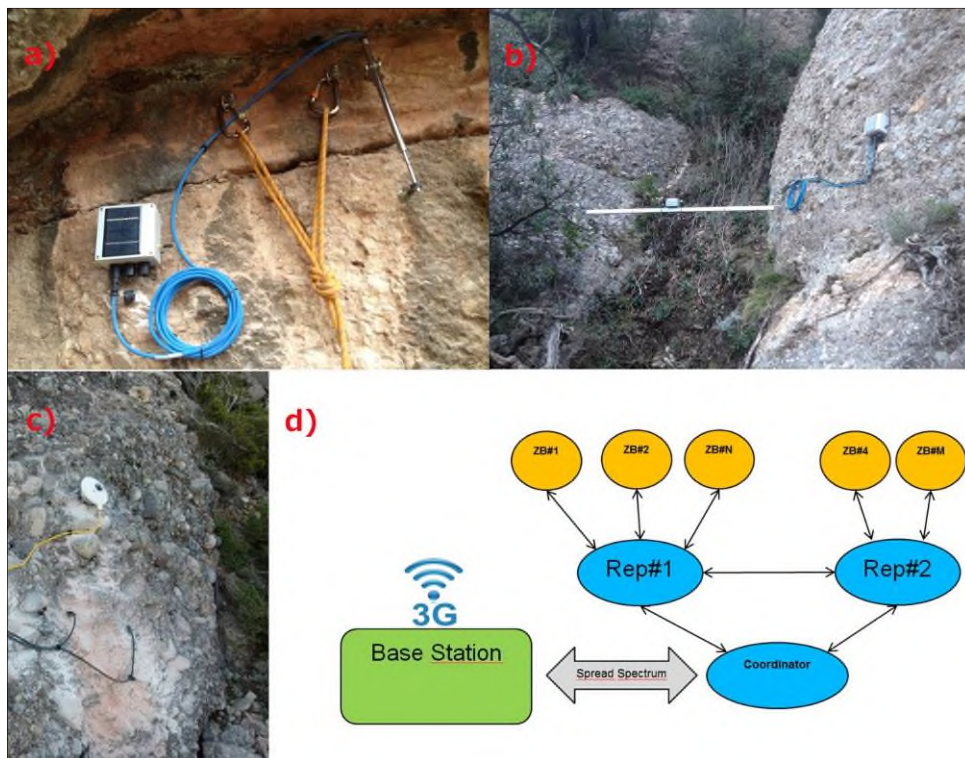

Figure 8. a) Crackmeter installed to measure distance between anchor points located at both sides of a crack, connected to a ZBLogger; b) Tiltmeter installed on a beam and connected to a ZBLogger; c) Soil temperature sensors and pyranometer installed on a face of the block cluster; d) Schema of the ZBLoggers network.

For a deep knowledge of the effect of temperature on the measure, besides a new air temperature sensor, two soil temperature sensors have been installed inside the rock at 20 cm and 40 cm depth near a pyranometer to measure solar (300 to 2800 nm) irradiance over the cluster of blocks (figure 8c). Also, a temperature sensor is installed at each of 4 beams.

To reduce the cost and effort of cabling sensors to one or several CS dataloggers, and the visual impact of it, a new concept of distributed wireless data acquisition network has been implemented, based on ZBLoggers. A ZBLogger is a low power, and low cost, system of ICGC own design with 3 single ended (or 1 differential plus 1 single ended) input channels and wireless connection, based on ZigBee protocols (IEEE 802.15.4 standard), which can communicate with others ZBLoggers and with CS datalogger as well. Eight LR6 1.5V rechargeable batteries and a solar cell of 0.96 W provides the system with enough energy for long term operation (5-10 years, depending of batteries service life in terms of charging cycles).

ZBLoggers digitize signal of input channels, at 1 sample each 10 minutes, with a 16 bits sigma-delta A/D converter. Data from a ZBLogger can be sent directly to a datalogger across the wireless network (800 m maximum in case of direct line of sight), or via others ZBLoggers acting as repeaters (figure 8d). Once data are stored inside the datalogger, they are sent to Data Centre via Internet, and archived into a database. Finally, "NetMon", a proprietary web based tool developed by ICGC, allows available data to be harnessed effectively. Currently, after 6 months without any important issue, the system remains operational and ready to be extended to others blocks during 2015.

2.3. Terrestrial Laser Scanner

The monitoring of several rock cliffs of Montserrat Mountain was carried out through an Ilris-3D (Optech) Terrestrial Laser Scanner (TLS) instrument also called Terrestrial LiDAR, which consists of a laser transmitter and receiver and a scanning device (figure 9). The laser beam is reflected directly onto the rock slope surface, which means that no reflector is necessary. The instrument computes the distance to an object, also called the range, by using the time-of-flight of the laser pulse [13]. According to specifications, ILRIS-3D can reach a maximum range of 700 m for natural slopes and decreases as a function of the material reflectivity and incidence angle to the object. The datasets acquired by this device can provide an accuracy of 7 mm at a distance of 100 m, according to the manufacturer's specifications. The device can acquire a huge number of points, also called point clouds, in a very short time (2,500 points/s), which provides a high density of information (around a few thousand points per square meter).

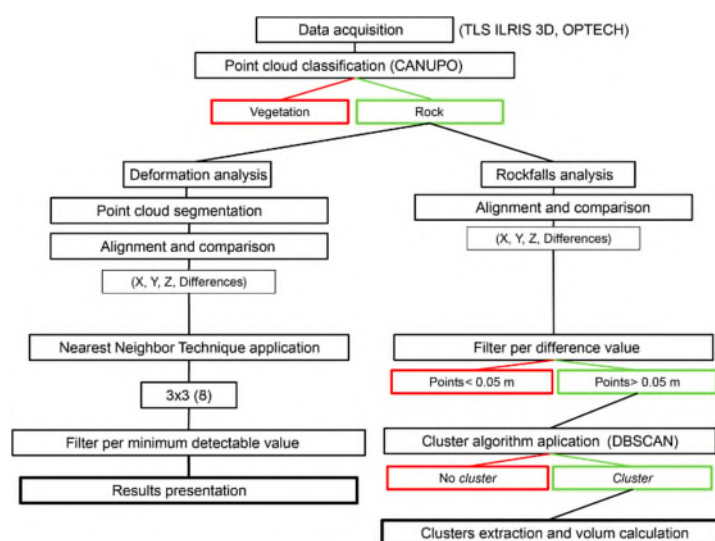**Figure 9.** Data acquisition with the TLS equipment in Montserrat Monastery cliff.

Figure 10. Workflow of the processes applied to detect deformation and rockfalls.

The time series of TLS data in Montserrat Mountain is the longest of all the techniques exposed in this work, so it has special interest in order to detect both rockfalls and deformation from years ago. In Degotalls area the first data acquisition was performed in May 2007 and 9 different fieldwork campaigns were conducted up to July 2014 (table 2). So, in this case the monitoring period span 2630 days. Degotalls study area consists of two different rock cliffs, so for the analysis this study area was separated into Degotalls North (N) and Degotalls East (E). Moreover, the first data acquisition of the Monserrat Monastery area was performed in February 2011 and 7 data acquisitions were carried out up to July 2014 (table 2), spanning a monitoring period of 1254 days. Firstly, a classification of each point cloud using CANUPO application [14] was performed in order to filter vegetation areas. Then, each dataset was aligned with the previous datasets to detect rockfalls between periods, or with the first dataset to detect accumulated deformations. This procedure was carried out through a preliminary identification of homologous points and a subsequent minimization of the distance between point clouds using the Iterative Closest Points (ICP) algorithm [15]. A refinement of the alignment was obtained through automatic outlier selection: those points with a distance greater than 3 cm were not included in the scan alignment process. The comparison of the different TLS datasets was based on the quantification of the distances between each pair of datasets and was performed using a conventional "point-to-surface distance" methodology implemented in IMInspect software, InnovMetrics PolyWorks v.10.0.

Table 2. Date of TLS acquisition and monitoring periods.

Monastery		Degotalls North		Degotalls East	
Date of acquisition	Cumulative days	Date of acquisition	Cumulative days	Date of acquisition	Cumulative days
		2007.05.11	0	2007.05.11	0
		2009.12.18	952	2009.12.18	952
2011.02.15	0	2010.12.02	1301	2010.12.02	1301
2011.05.12	86	2011.05.12	1462	2011.05.12	1462
2011.12.12	300	2011.12.12	1676	2011.12.12	1676
2012.03.28	407	2012.03.28	1783	2012.03.28	1783
2012.06.22	493	2012.06.22	1869	2012.06.22	1869
2012.11.06	630	2012.11.06	2006	2012.11.06	2006
2013.12.11	1030	2013.12.11	2406	2013.12.11	2406
2014.07.23	1254	2014.10.07	2706	2014.07.23	2630

In order to detect rockfalls or deformation, two different processes were applied (figure 10). In the case of deformation, a Nearest Neighbour (NN) filtering technique [7] was applied in order to improve the accuracy of the scans comparison. Briefly, this technique involves the extraction of the differences between successive scans and the median computation of the NN (NN = 8 in this study). As a result of this process the minimum detectable deformation value was 1 cm. On the other hand, to detect rockfalls a procedure to find clusters was applied [16]. Mainly this process consists of three steps: a) filtering of differences not corresponding to rockfalls; b) application of DBSCAN algorithm (Density-Based Spatial Clustering of Applications with Noise [17]) to remove noise and find different clusters; and c) quantification and volume computation of the single clusters detected corresponding to single rockfalls. Given that the minimum value of used differences was 5 cm, the minimum number of required points of a cluster was defined as 10 and the average point spacing of the scans was between 7 cm and 9 cm, the minimum detectable rockfall volume was defined as 0.001 m^3 (equivalent to 2.5 kg of conglomerate).

2.4. GBSAR

In 2014-2015 a first extensive measurement campaign using a Ground Based Synthetic Aperture Radar (GBSAR) has been performed in Montserrat. Data collected by this kind of SAR sensors allow obtaining terrain reflectivity images, which can be processed by means of differential SAR interferometry (DInSAR) algorithms for the monitoring of deformation episodes, with millimetric accuracy [18] and [19]. DInSAR techniques are based on the use of the phase-differences between multitemporal pairs of complex SAR images of the same area of study, to obtain the terrain displacement undergone in the line-of-sight (LOS) direction.

The aim of the experiment was to take advantage of the wide area coverage (2 km long by 1 km wide) and its high sensitivity to displacement detection (on the order of millimeter). GBSAR sensors are used for the precise monitoring of small-scale phenomena. These kind of instruments have been used for several applications as landslide monitoring, subsidence hazards in urban areas, volcanoes monitoring, etc, [20] and [21], when a classical Orbital DInSAR systems cannot be used because of the bad geometric orientation of the scenario or the revisit time of the Spaceborne sensor is not short enough to monitor the deformation. The main characteristics of the UPC RiskSAR (GBSAR) are summarized in table 3.

Table 3. Main characteristics of RiskSAR equipment (GBSAR system of UPC).

Parameters	**Values**
Carrier Frequency	9,65 GHz
Modulation	triangular CW-FM
Signal bandwidth	100MHz
Polarization	Full polarimetric combinations
range resolution	1,5 m
azimuth resolution	10 mRad
range coverage	1,5Km
azimuth coverage	±30º

The instrument was placed in el Pont de Guilleumes (figure 11), at 380m altitude, its orientation was south and 25º upslope, pointing to two different main rock cliffs, 400 and 800 meters far from the radar. The system operated autonomously but it could be remotely controlled via wireless link. A sequence of 1 measurement per hour was programmed along the 5 months experiment (October 2014 - February 2015).

Figure 13 shows the reflectivity image covered by the sensor projected on topography. From the image, it can be observed the strong reflectivity response corresponding to the main rock cliffs. Different radar calibrators were deployed along the slope to facilitate the image geocoding process. A test with a Polarimetric Active Radar Calibrator (PARC) over a millimetric positioner was performed to validate system capability to detect small displacements (figure 12). Small difference between real and retrieved position can be seen, which are due to thermal stabilization of the internal electronics of the PARC.

Figure 11. RiskSAR system placed at Pont de Guilleumes site with weatherproof cover for temporary use at short term.
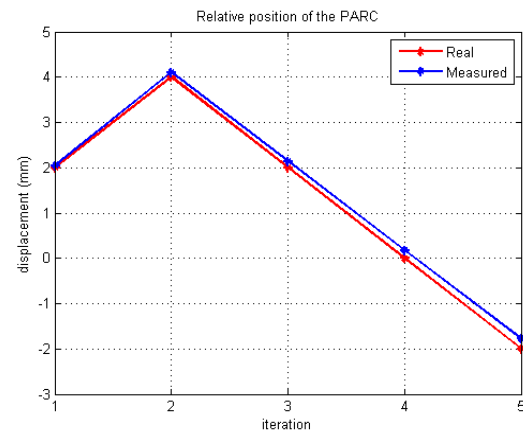

Figure 12. PARC displacement position retrieved after DInSAR processing.
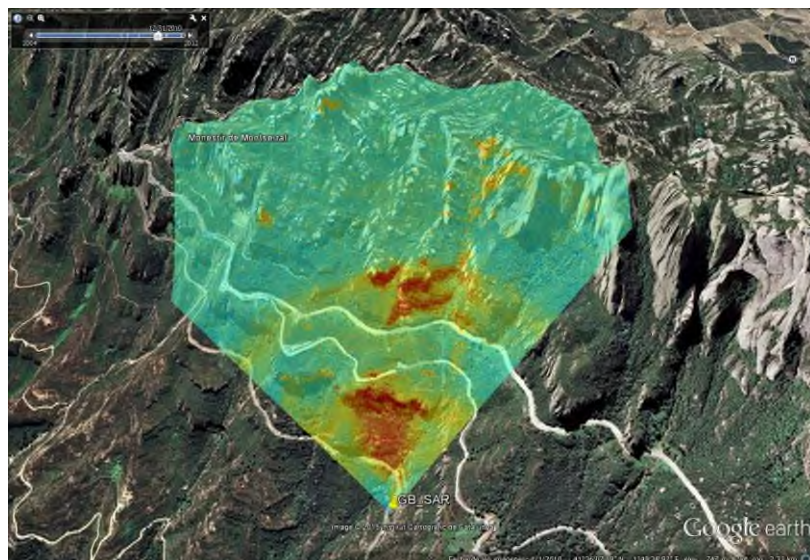

Figure 13. Radar reflectivity image on Google Earth map of the scenario.

For this type of sensors, the atmospheric phase screen (APS) is the most relevant artefact of distortion on the interferometric phase. Hence, in order to apply any DInSAR technique to obtain reliable deformation maps, these atmospheric artefacts must be correctly estimated and consistently compensated for [22] and [23]. Unfortunately it implies that an important set of measurements have to be discarded because the accentuated atmospheric anomalies in mountainous areas as fog, rain, stratification and temperature inversion.

3. Preliminary results and analysis
As corresponding to pilot tests phase, the results obtained until now are only considered as preliminary, pending on reviewing, adjustment or improvement. The interpretation of an eventual rock mass movement is expected to be a combination of: temporary and retrievable displacements as the elastic response to thermal effects and variable actions under failure threshold; and permanent

cumulative displacements as the plastic signs of progress of failure. This distinction corresponds to the next subsections, preceded by another particular result obtained by the monitoring works.

3.1. Rock fall activity assessment

TLS allows the detection of rockfalls that were not recorded by classical observational tasks, and also to calculate their volume. On the contrary, GBSAR is not able to clearly detect these rapid changes on scenery, because the comparison in terms of the signal's phase. All these unobserved events were characterized by small magnitude, ranging volumes between 0.001 and 0.732 m^3, and associated with pebbles disaggregation and small slabs failure. The rockfalls detected by period could be observed in table 4. In the case of Monastery cliff the total number of rockfalls detected was 44; ranging volumes between 0.001 and 0.45 m^3 (90% of rockfalls minor than 0.05 m^3). In this area, a remark has to be done in the results of periods between June 2012 and December 2013, because some of the detections were derived from the stability tasks carried out in a certain rock block.

Table 4. Rockfall activity characterized with Terrestrial TLS expressed in number of rockfalls detected per period of analysis in each study area.

Monastery		Degotalls North		Degotalls East	
Period	Rockfalls	Period	Rockfalls	Period	Rockfalls
		2007.05–2009.12	11	2007.05–2009.12	18
		2009.12–2010.12	22	2009.12–2010.12	33
2011.02–2011.05	0	2010.12–2011.05	8	2010.12–2011.05	8
2011.05–2011.12	3	2011.05–2011.12	16	2011.05–2011.12	8
2011.12–2012.03	2	2011.12–2012.03	8	2011.12–2012.03	9
2012.03–2012.06	1	2012.03–2012.06	1	2012.03–2012.06	0
2012.06–2012.11	13	2012.06–2012.11	9	2012.06–2012.11	4
2012.11–2013.12	21	2012.11–2013.12	8	2012.11–2013.12	7
2013.12–2014.07	4	2013.12–2014.10	6	2013.12–2014.07	4
Total	44	Total	89	Total	91

On the other hand, the specific results of Degotalls N and E could be also observed in table 4. In order to detect just the unobserved rockfalls, in Degotalls N a filtering of the events caused by the big rockfall occurred in December 2008 had to be carried out. Thus the final results showed a total number of rockfalls of 78; ranging volumes between 0.001 and 0.73 m^3 (90% of rockfalls minor than 0.1 m^3). In the case of Degotalls E the total number of rockfalls recorded was 91; ranging volumes between 0.001 and 0.28 m^3 (95% of rockfalls minor than 0.1 m^3). As an example of results, the rockfalls detected in Degotalls E rockface are presented in figure 14a, as well as their evolution over time (figure 14b) and their volume histogram (figure 14c).
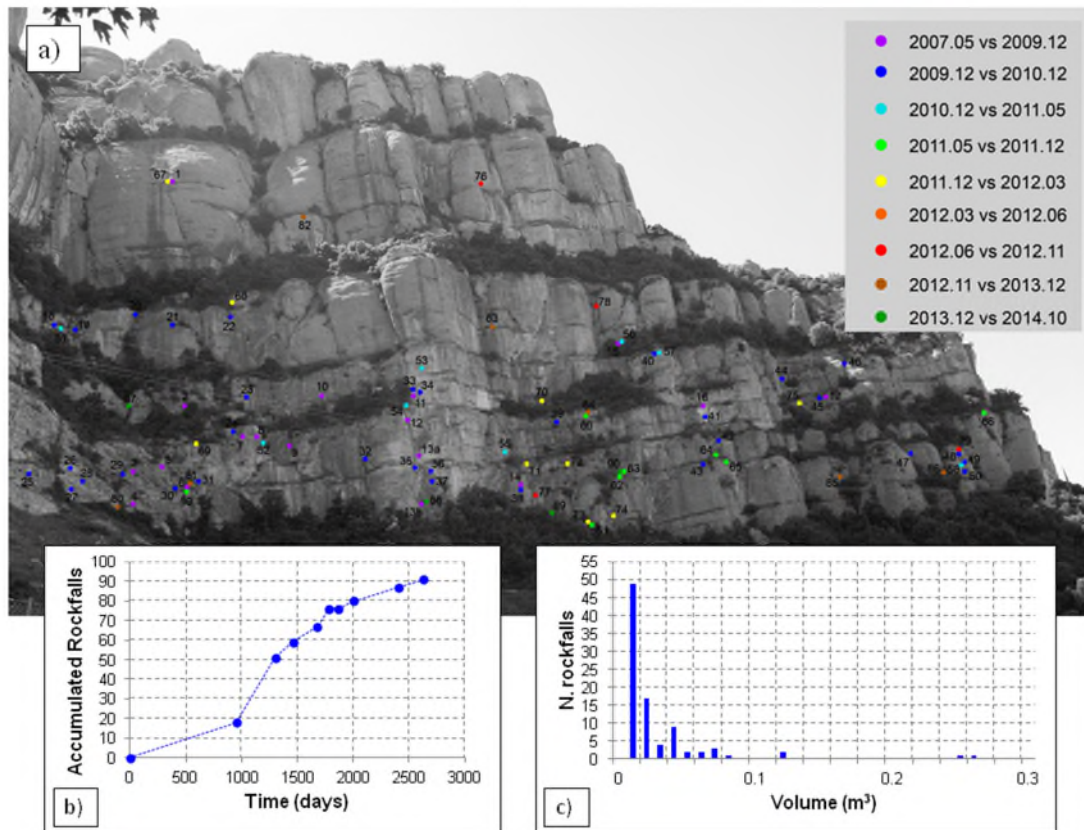
Figure 14. a) Rockfalls in Degotalls E rockface; b) Rockfalls evolution over time; c) Rockfall volume histogram.

Rate of activity seems to be uniform during time but the low time resolution of TLS data does not seem to be the most appropriate. So, for 2015 it is planned to increase the sampling frequency to seasonal control, to check time variability.

3.2. Rock mass elastic/temporal deformation

The register of the monitoring of rock joints in block A3-6 during 4 years (but with some gaps due to technical problems with wildlife interaction) clearly show the annual cycle and also daily oscillation (figure 15), as it can be clearly identified with a FFT analysis. This behaviour can be linked with thermal deformation of rock mass superficial part, including the analysed block, but also thermal effect on sensor must be considered. The mean amplitude of annual oscillation is 1.7, 0.9 and 1.3 mm for sensors 1, 2 and 3 respectively, and 34.6ºC for temperature (figure 15). Sensor 2 and 3 show a completely elastic behaviour recovering the displacement after annual cycle, but for the sensor 1 (a wire extensometer measuring the aperture of the rear joint at the upper part) a slight tendency to accumulate displacement at a rate of 0.33 mm/year can be seen. This fact must be confirmed with longer time-series to determine if it could be a creeping process conducting to a long-term toppling failure.
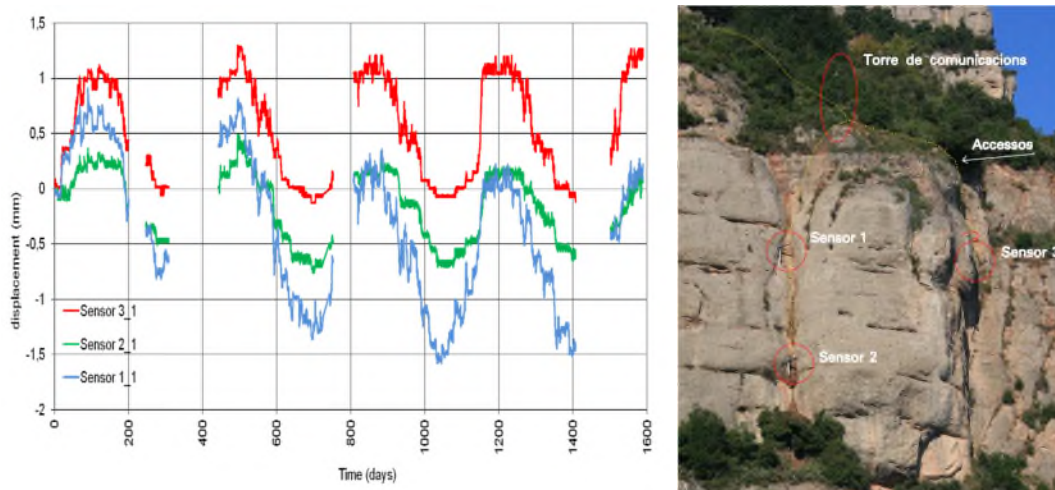
Figure 15. 4-years long register of monitoring of rock joints in block A3-6, where sensors 1 and 2 are wire extensometers orthogonal to joint, and sensor 3 is a bar extensometer parallel to joint.

Thermal effect on sensors is expected to be mainly related with air temperature with rapid heat transfer, whereas the rock mass response should be related to the temperature of the ground. To improve the knowledge in this issue, in the new instrumented block (Diable) thermometers for the air and inside the rock (at depths of 20 and 40 cm) have been installed, as well as a pyranometer (because the sun radiation influences the rock temperature). After the first 3 months of monitoring, the heat flux inside the rock mass is clearly shown in the figure 16, but the data are just starting to be analysed.
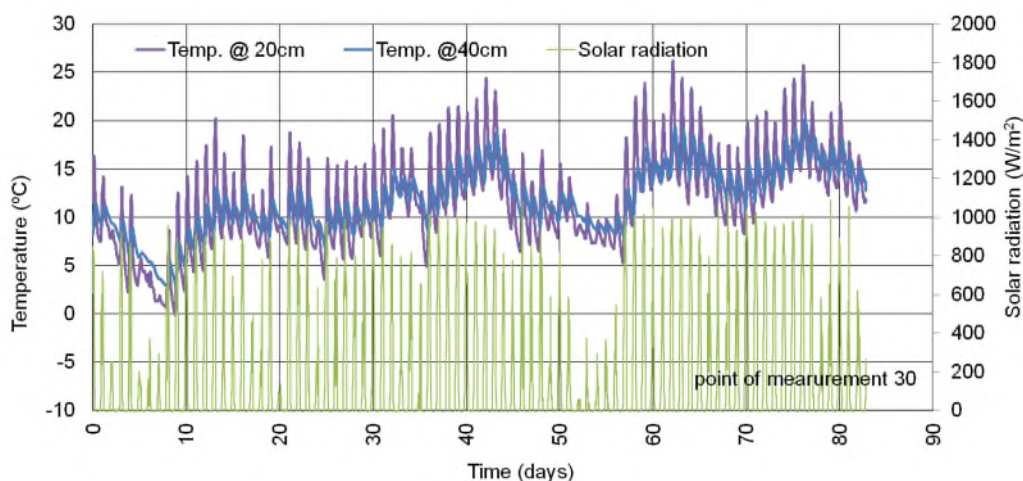

Figure 16. Register for the 3 first months in Diable block: temperature inside the rock mass at 20 and 40 cm, and solar net radiation.

The other monitoring techniques, at present, are not giving a clear result for this level of rock mass deformation. Probably this range of movement (mm level) is under the error for the equipment and site implementation. Under the working conditions, at present we are reaching precisions about 10 mm for TLS, 3 mm for GBSAR and 1 mm for Total Station. Depending on the magnitude of displacement of each rock block related with its structural disposal, the movement will be detected or not with a given technique. For instance, at the Cadireta we plan to complete an annual cycle with seasonal measurements with Total Station priori to drive any conclusion. To improve the precision of both scanning techniques, for 2015 a new test with GBSAR at closer distances and higher frequency in the

Monastery cliff is planned; on the other hand, 2 points for positioning TLS will be added closer to both sectors under deformation analysis.

3.3. Rock mass plastic/permanent deformation

On the detection of precursory deformation, TLS monitoring was able to detect movement in two different blocks located in Degotalls N study area (figure 17). The Block A instability was detected in the period 2007.05vs2009.12, after the big event occurred on December 2008 and next to the fallen block. This movement was characterized by an initial mean displacement of 2 cm and a subsequent stop in the following periods. This behaviour suggests that the movements were caused by the great rockfall occurred on December 2008; in the following periods the displacement stopped because of the appropriate stabilization works carried out on the same block.
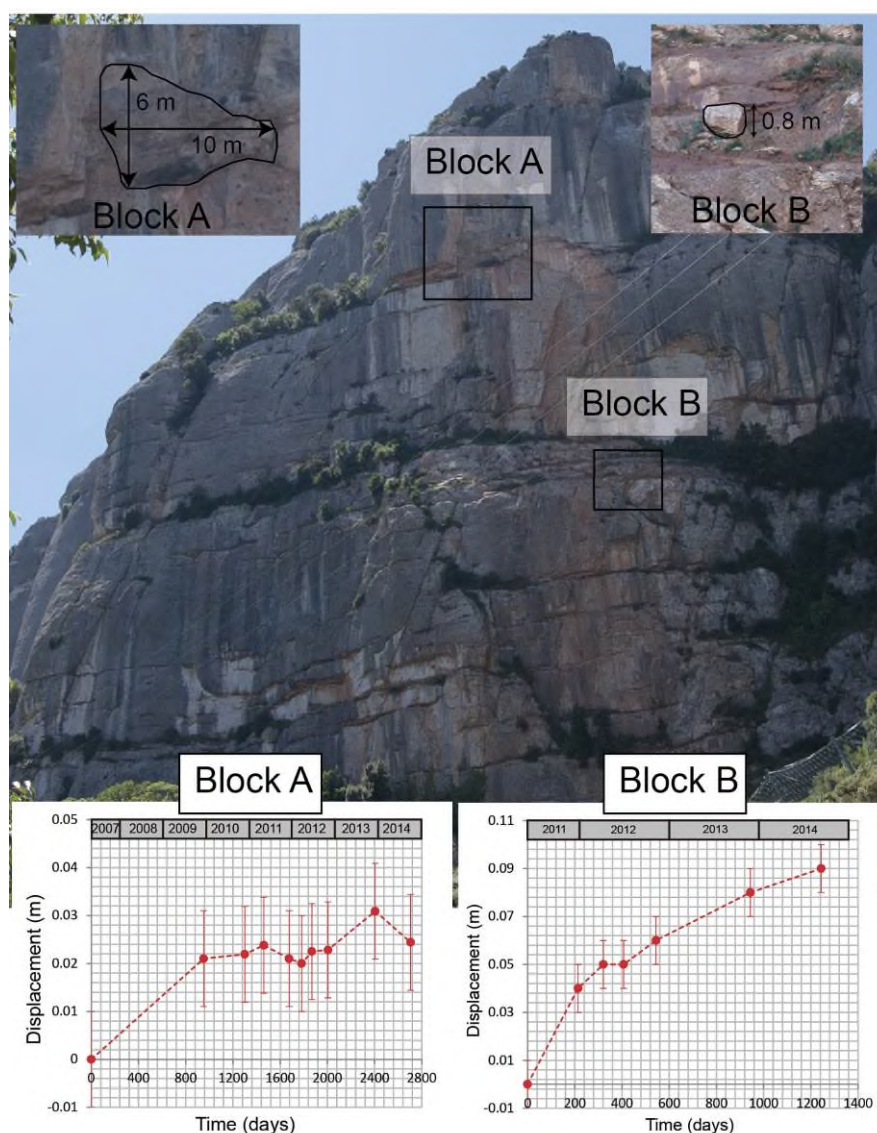

Figure 17. Location of the two blocks where displacement has been detected and their evolution over time, as measured with TLS.

The second instability (Block B) was detected in the period 2011.05vs2011.12 in a block close to a small rockfall occurred in the same period. An initial mean movement of 4 cm was detected and in this

case any stabilization tasks were performed so an increment of the displacement has been recorded (figure 17). Until July 2014 the accumulated displacement in this block was 9 cm showing the need to continue with the monitoring surveys, although the TLS seasonal frequency makes difficult to use it as a prevention tool. Fortunately, there is a rockfall fence protecting the road. The total amount of displacement that the block will be able to accumulate before falling will depend on the particular stability conditions of the block; for hard rock massif and isolated rockfall detachment, it is expected to be small [24].

For 2015 it is planned to add several surveying prisms for the block A to contrast the TLS measures with Total Station technique (with slightly higher precision), ultimately to confirm the proper response of the stabilization works. In parallel the feasibility of continuous instrumentation is under analysis.

Finally, for the pilot test of GBSAR at Guilleumes, the displacement map retrieval of the rock cliffs can be carried out with the zero baseline adaptation of the CPT technique [20]. Figure 18 shows a preliminary result obtained using a daily dataset of 34 SAR images. Non significant displacements are observed on the surface of the rock cliffs, showing a stable behaviour during the measurement campaign.
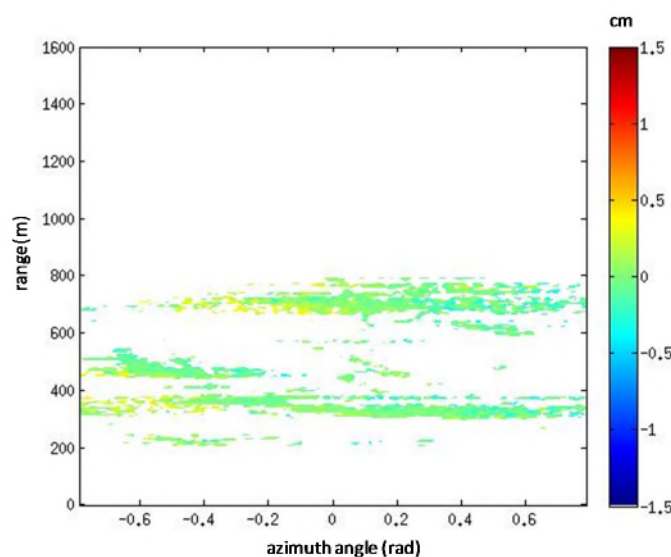

Figure 18. Displacement map (in polar coordinates) retrieved after DInSAR processing. Non significant displacements are observed by the moment.

4. Conclusions

We are on the way to improve our knowledge on the behaviour of the rock mass in Montserrat Mountain and the comprehension of the geomechanical processes leading to rockfall failures. One of the main difficulties to reach this goal is its stiff/brittle behaviour, so it is necessary to achieve the best precision in measurement. However, the applied monitoring techniques are giving first interesting results in this sense. Preliminary observations show two kinds of movements: centimetric displacements in blocks with apparent high instability without detachment, that confirms our hope to be able to analyse premonitory signs of rupture; and millimetric displacements in joints as a daily/seasonal cyclic response, for which it is necessary to determine the thermo-mechanical coupling in the next future.

At the same time, these techniques let us to accurately quantify the rockfall activity, being the TLS a valuable tool to detect the unnoticed rockfall. These data are very useful to assess the magnitude-frequency relationship for a proper hazard assessment.

The different monitoring techniques are providing coherent results, according to each time-series length and increasing experience on its application in Montserrat. Taking into account the best capabilities of each technique, the results show an excellent complementarity of the four techniques that should be explored in deep. After these separate tests, it is planned to establish Monastery cliff (and secondly Degotalls) as pilot master area for the integration of the different techniques for a cross check vision.

References
[1]　Alsaker E, Gabrielsen RH and Roca E 1996 The significance of the fracture patterns of Late-Eocene Montserrat fan-delta, Catalan Coastal Ranges (NE Spain) *Tectonophysics* 266 465–91

[2]　Fontquerni S, Vilaplana JM, Guinau M, Royán MJ, Barberà M, Janeras M 2012 Los elementos vulnerables expuestos a los desprendimientos de rocas en Montserrat *VIII Congreso Geológico de España* (Oviedo)

[3]　Palau J, Janeras M, Prat E, Pons J, Ripoll J, Martínez P and Comellas J 2011 Preliminary assessment of rockfall risk mitigation in access infrastructures to Montserrat *Second World Landslide Forum* (Rome)

[4]　Royán MJ and Vilaplana JM 2012 Distribución espacio-temporal de los desprendimientos de rocas en la montaña de Montserrat Cuaternario y Geomorfología 26 **1–2** 151–70

[5]　Janeras M, Palau J, Prat E, Pons J, Rodríguez H, Martínez P and Comellas J 2013 Valoración de 10 años de mitigación del riesgo de caída de rocas en el Cremallera de Montserrat *VIII Simposio Nacional sobre Taludes y Laderas Inestables* (Palma de Mallorca: ed E Alonso, J Corominas and M Hürlimann)

[6]　Janeras M, Palau J, Prat E and Ripoll J 2011 Montserrat: on a long way to rock fall risk mitigation – First experiences, some lessons and future perspectives *Interdisciplinary Rockfall Workshop* (Innsbruck – Igls: RocExs)

[7]　Abellán A, Jaboyedoff M, Oppikofer T and Vilaplana JM 2009 Detection of millimetric deformation using a terrestrial laser scanner: experiment and application to a rockfall event *Nat. Hazards Earth Syst. Sci.* **9** 365–72

[8]　Royán MJ, Abellán A, Vilaplana JM 2015 Progressive failure leading to the 3 December 2013 rockfall at Puigcercós scarp (Catalonia, Spain) *Landslides* DOI 10.1007/s10346-015-0573-6

[9]　Arosio D, Longoni L, Papini M, Scaioni M, Zanzi L and Alba M 2009 Towards rockfall forecasting through observing deformations and listening to microseismic emissions *Nat. Hazards Earth Syst. Sci.* **9** 1119–31

[10]　Royán MJ, Abellán A, Jaboyedoff M, Vilaplana JM and Calvet J 2014 Spatio-temporal analysis of rockfall pre-failure deformation using Terrestrial LiDAR *Landslides* **11** 697-709

[11] Cabranes, F 2015 *Estudio geomecánico de la estabilidad de la Cadireta d'Agulles (Montserrat)* (*Unpublished* B.Sc.Degree Thesis, ETSECCPB, Technical University of Catalonia) p 156

[12] Gallach X 2012 Estudi de susceptibilitat de caiguda de roques a la paret del Monestir de Montserrat a partir de la inspecció d'indicadors d'inestabilitat i d'anàlisi SIG (*Unpublished* M.Sc.Degree Thesis, UB, University of Barcelona) p 32

[13] Petrie G and Toth CK 2008 Introduction to laser ranging, profiling and scanning *Topographic Laser Ranging and Scanning: Principles and Processing* ed J Shan and CK Toth (London: CRC Press / Taylor & Francis) pp 1–28

[14] Brodu N and Lague D 2012 3D terrestrial LiDAR data classification of complex natural scenes using a multi-scale dimensionality criterion: Applications in geomorphology *ISPRS J. Photogrammetry and Remote Sensing* **68** 121–34

[15] Chen Y and Medioni G 1992 Object modelling by registration of multiple range images *Image Vis. Comput.* **10** 145–55

[16] Tonini M and Abellán A 2014 Rockfall detection from LiDAR point clouds: a clustering approach using R *J. Spatial Information Sci.* **8** 95–110

[17] Ester M, Kriegel H, Sander J and Xiaowei Xu X 1996 A density-based algorithm for discovering clusters in large spatial databases with noise *Proc. 2nd Int. Conf. on Knowledge Discovery and Data Mining*

[18] Gabriel AK, Goldstein RM and Zebker HA 1989 Mapping small elevation changes over large areas: Differential radar interferometry *J. Geophys. Res.* vol. 94 **B7** 9183

[19] Massonnet D and Feigl KL 1998 Radar interferometry and its application to changes in the Earth's surface *Rev. Geophys.* vol. 36 **4** 441

[20] Iglesias R, Aguasca A, Fabregas X, Mallorqui JJ, Monells D, López-Martínez C and Pipia L 2015 Ground-Based Polarimetric SAR Interferometry for the Monitoring of Terrain Displacement Phenomena–Part I: Theoretical Description *IEEE Journal of Selected Topics in Applied Earth Observations and Remote Sensing* **8** 980–93

[21] Iglesias R, Aguasca A, Fabregas X, Mallorqui JJ, Monells D, López-Martínez C and Pipia L 2045 Ground-Based Polarimetric SAR Interferometry for the Monitoring of Terrain Displacement Phenomena–Part II: Applications *IEEE Journal of Selected Topics in Applied Earth Observations and Remote Sensing* **8** 994–1007

[22] Pipia L, Fabregas X, Aguasca A and Lopez-Martinez C 2008 Atmospheric artifact compensation in ground-based DInSAR applications *IEEE Geosci. Remote Sens. Lett.* **5** 88–92

[23] Iglesias R, Fabregas X, Aguasca A, Mallorqui JJ, López-Martínez C, Gili JA and Corominas J 2014 Atmospheric phase screen compensation in ground-based SAR with a multiple-regression model over mountainous regions *IEEE Trans. Geosci. Remote Sens.* **52** 2436–49

[24] Janeras M, Macau A, Figueras S and Comellas J 2010 Prevention and control of rocky slope instabilities induced by blasting vibration in tunneling – application to Núria rack railway *Rock Mechanics in Civil and Environmental Engineering* (Lausanne: ed J Zhao, V Labiouse, JP Dudt, JF Mathier EUROCK 2010)